Nonadiabatic Forces in Ion-Solid Interactions: The Initial Stages of Radiation Damage

Alfredo A. Correa
Lawrence Livermore National Laboratory, Livermore, California, 94551, USA

Jorge Kohanoff
Department of Physics and Astronomy, Queen's University, Belfast BT7 1NN, United Kingdom

Emilio Artacho
Nanogune and DIPC, Tolosa Hiribidea 76, 20018 San Sebastían, Spain
Basque Foundation for Science, Ikerbasque, 48011 Bilbao, Spain
Cavendish Laboratory, University of Cambridge, Cambridge CB3 0HE, United Kingdom

Daniel Sánchez-Portal
Centro de Física de Materiales (CFM-MPC) CSIC-UPV/EHU and DIPC, Paseo Manuel de Lardizabal 5, 20018 San Sebastián, Spain

Alfredo Caro
Los Alamos National Laboratory, Los Alamos New Mexico 87545, USA
(Received 2 February 2012; published 21 May 2012)

The Born-Oppenheimer approximation is the keystone for molecular dynamics simulations of radiation damage processes; however, actual materials response involves nonadiabatic energy exchange between nuclei and electrons. In this work, time dependent density functional theory is used to calculate the electronic excitations produced by energetic protons in Al. We study the influence of these electronic excitations on the interatomic forces and find that they differ substantially from the adiabatic case, revealing a nontrivial connection between electronic and nuclear stopping that is absent in the adiabatic case. These results unveil new effects in the early stages of radiation damage cascades.

DOI: 10.1103/PhysRevLett.108.213201 PACS numbers: 34.50.Bw, 31.30.−i, 34.20.−b, 61.85.+p

When an energetic particle collides with a solid target it deposits energy on the nuclei and on the electrons of the host material. For particle velocities below the Fermi velocity of the target, nuclear and electronic stopping are both relevant, and the result of the interaction is a collision cascade [1]. A full understanding of these early stages of radiation damage provides knowledge and tools to manipulate them to our advantage, not only on materials for nuclear applications but also on materials related to the space industry, novel processing techniques using lasers and ions, and the large field of assessing the effects of radiation on living tissues, both for understanding damage and for therapeutic use.

Within the condensed matter community, and since the pioneering speculations about the multiple effects that a collision cascade produced by an energetic particle would introduce in a solid target [2], the interest in knowing in detail the complexity of this highly nonequilibrium process has fueled a huge amount of research, both experimentally and by using computer simulations aiming at understanding radiation damage in matter [3].

During the 1980s, the advent of powerful computers allowed Averback and collaborators to study, for the first time, the radiation damage on a target with a number of atoms large enough to contain the main stages of collision cascades [4]. This early work unveiled the transition from ballistic to thermal phase of the cascade and the liquid-like nature of the latter when significant damage recovery occurs as it quenches down. Simultaneously, the development of a series of many-body classical interatomic potentials [5,6] allowed us to reproduce in detail and at low computational cost a number of properties of solid targets, in particular the energetics of perfect and defected crystals, elastic constants, and thermodynamic properties such as melting temperature and latent heat, all contributing to increased knowledge of the properties of the damaged state of the target. These works, however, lacked an essential component, namely the dynamic response of the electrons to such a large perturbation. This is because the majority of radiation damage research in material science was done within the Born-Oppenheimer (BO) or adiabatic approximation [7], where electrons adjust instantaneously to moving nuclei, completely ignoring their dynamics. The BO approximation is the keystone to the atomistic molecular dynamics (MD) simulations, with both *ab initio* or empirical interatomic force fields. From the early days of the MD approach to describe radiation damage until now, authors noticed the practical necessity to go beyond this approximation, ranging from collision cascades [8–17] and rapid shocks [18] to current-induced forces [19].

In parallel, the electronic structure community has been studying the problem of electronic stopping power (S_e), where the quantum mechanical nature of the electronic

response is taken into consideration through different levels of approximation, ranging from Thomas-Fermi [20], shell models [21], Hartree-Fock [22], Density Functional Theory (e.g., for the homogeneous electron gas [23,24], within the linear dielectric response approximation [25]), to semiclassical nonadiabatic atom-atom collisions (e.g., using Firsov's model [26,27]). The main focus of this community is on the projectile energy-loss mechanism through the electronic system.

Electronic stopping is one of the components of the entire process; there are two other elements equally important for a complete picture of a radiation damage event, which are beyond the scope of this Letter: (1) As electrons get energy from projectiles via stopping, they become excited and this energy is spread by transport processes until it eventually becomes electronic thermal energy. (2) The electron-phonon interaction is responsible for the recovery of thermal equilibrium between the nuclear and the electronic subsystems.

Hybrid models combine different aspects of the problem in an *ad hoc* manner; these include two-temperature models [8,9], phenomenological stopping based in the local density [10], collective excitations in a Coulomb explosion [11–14], and thermal spike approaches [8,9,15,16]. Perhaps the most sophisticated approach at present is the extension of Ref. [10] to include the electronic component as a classical field coupled to the nuclei via heat transport equations [17].

The aims of this Letter are to interconnect the two, so-far disconnected, aspects of the same process, the electronic and nuclear loss mechanisms via *ab initio* simulations that take into account the electron dynamics of the system, and to depict what happens to the nuclei when the electrons are excited by a fast-moving particle in the target material.

In this work we apply the formalism of time dependent density functional theory (TDDFT) to model the electron dynamics in the first stages of the energy deposition. We analyze the ability of the method to calculate the electronic stopping power (S_e) for metals, comparing the accuracy of the simulation results with those contained in the SRIM (formerly TRIM) database [28,29] for the case of H in Al. We also analyze the nature of the time dependent forces experienced by the atoms as the projectile moves along its trajectory. Our work follows that of Pruneda and others on nonadiabatic dynamics in insulators [30,31] but unveils one of the most fundamental consequences of the nonadiabaticity of the electron-nuclear system, namely the modification of the interatomic forces that result from the perturbation of the electronic system.

The main simulations consist in forcing the movement of a projectile (proton) in the metallic bulk, which mimics a highly energetic particle as it enters the material. Calculations are performed using SIESTA [32], modified [33] to implement the solution of Time Dependent Kohn-Sham (TDKS) orbitals via a semi-implicit Cayley form integrator [34] (also called Crank-Nicholson [35]). Kohn-Sham electron orbitals, expanded in a local polarizable (double-zeta plus polarization, or DZP) basis around the atoms (including the projectile atom), are evolved in time with a self-consistent Hamiltonian that is a functional of the density. The local-density approximation (LDA) functional is used for the presented Al calculations [36]. To augment the basis, we also include a dense set of manually added (ghost) hydrogenic orbitals around the projectile's trajectory.

We use a periodic cell with 64 host Aluminum atoms plus a proton, represented by a Troullier-Martins pseudopotential (3 valence electrons per Aluminum atom are explicitly considered) and a $2 \times 2 \times 4$ k-point grid to sample the Brillouin zone. The density is sampled with a 150 Ry mesh cutoff.

We perform the TDDFT calculation on the electronic system at given time-dependent nuclear positions, under two simplifying assumptions: (i) the host (target) atoms are fixed in the equilibrium positions and (ii) the projectile is subject to a rectilinear uniform movement along a channeling $\langle 100 \rangle$ trajectory (that maximally avoids collisions with the host atoms) and also off-center channeling trajectory (that is, parallel to channeling but halfway toward a row of host atoms in order to assess sensitivity to the perfect channeling conditions). The initial condition of the electronic system is taken to be that of the ground state with a projectile at the initial position. The time step of the TDDFT simulation is chosen to be inversely proportional to the velocity of the projectile, such that the spatial resolution on the projectile position is constant among simulations at different velocities. The time step is always below 3 attoseconds, which is the stability limit for the numerical time-integration scheme with the chosen type of basis set.

Under these conditions, the externally forced movement of the projectile (assumed to have some constant velocity or momentum) will produce an overall increase on the total energy. After the projectile covers some distance, the total energy of the system increases at a steady rate (apart from oscillations) and therefore a stationary state is reached (Fig. 1). The oscillations reflect the periodicity of the Al lattice.

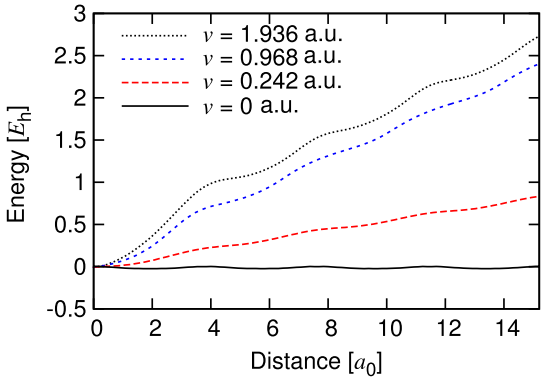

FIG. 1 (color online). Proton in aluminum: Total (Kohn-Sham) energy increase as a function of position for different proton projectile velocities. Lattice atoms are fixed as its equilibrium positions while projectile passes in a $\langle 100 \rangle$ channelling trajectory at velocity v. The average stationary slope (determined for projectile positions larger than $\sim 5a_0$) is used to calculate the stopping power (Fig. 2).

The slope of total energy vs. projectile position gives the nonconservative force that, in the real system, would be associated with energy loss of the projectile, or equivalently, the energy gained by the target. The above assumptions (i) and (ii) are justified for a channeling orientation since during the short simulated time (relative to the nuclear motion), the position of the host atoms in the supercell would move insignificantly and also because the relative velocity change of the projectile would be negligible. In addition, this method of calculating the stopping is consistent with the definition of *electronic-only* stopping power (i.e., as a separate contribution from the nuclear stopping, dominant at low projectile velocities).

Fig. 2 shows electronic stopping power versus proton velocity, together with SRIM data. The results are also consistent with the analysis provided by velocity-dependent potentials in Ref. [37]. For the channeling direction, the prediction is below SRIM data; this result is in part expected for various reasons. First, the projectile passes through the center of the channel. Secondly, in our simulations we only consider explicitly valence electrons, leading to an underestimation above $v \sim 2.5$–3 a.u.. An additional factor might be the use of a local (in time) exchange-correlation functional, as retarded exchange-correlation effects are know to create additional frictional forces, as analyzed for low velocities in Ref. [38]. As expected, a parallel off-center channeling trajectory increases the value of stopping, bringing it in better agreement with the SRIM data. The unavoidable basis-size and finite-system-size effects introduce additional deviations ($v \sim 0.5$–1 a.u.) which, however, do not affect the main conclusions of our work. Taken into account the limitations mentioned, these results show the power of the TDDFT technique to accurately reproduce electronic stopping power in realistic systems.

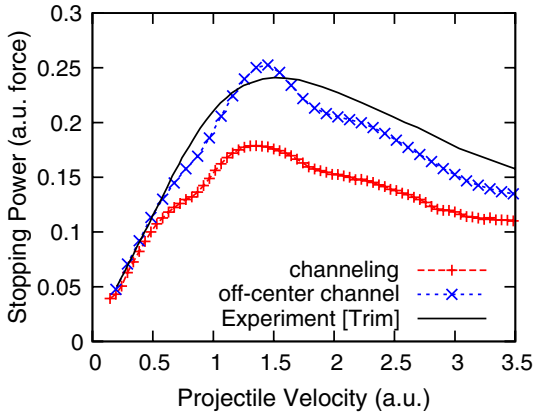

FIG. 2 (color online). Proton in aluminum stopping power: average stopping power (S_e) vs. projectile velocity v for a channeling trajectory (pluses) and for an off-center channeling trajectory parallel to the former (crosses). Continuous line refers to the nominal tabulated result from the SRIM/TRIM database [28,29], whose multiple fitting data sources have a spread of ~10% [41].

Now we turn to the relationship of these results with the radiation damage problem. Ever since the beginning of the large-scale computer simulations of radiation damage, a great interest was devoted to the analysis of the differences between Coulomb explosion and thermal spike induced by swift (heavy) ions in the metals. For a review, see [3]. There are two ways to analyze this phenomenon, the band picture and the ionization picture.

In the band picture, when electrons are excited in a metal, the band contribution to the cohesive energy decreases due to the population of antibonding states, while the nuclear plus core Coulombic repulsion remains unchanged, giving rise to a net repulsion between the nuclei. For a swift projectile creating an ion track, this gives rise to a collective radial-out force of host nuclei along the track. In the ionization picture, electrons are ejected away from the atoms close to the projectile trajectory, creating positively charged ions.

The Coulomb explosion model then considers that the potential energy is subsequently converted into atomic motion [11–14]; this conversion depends on the lifetime of the space charge, which is governed by the response time of the electron gas in the system, roughly the inverse of the plasma frequency (~ femtoseconds). In spite of this short duration, the ionized atoms located around the projectile trajectory acquire kinetic energy, which could reach several eV. This coherent (in space and time) transfer of energy can have noticeable effects, as it results in (1) the generation of a shock wave that may favor phase transformations in materials with allotropic forms and/or (2) a strong excitation of soft phonon modes. If soft modes are present, large amplitude displacements may be induced even with relatively small energies, thus favoring disorder and defect formation.

The energy transfers per atom involved in the Coulomb excitation process are much smaller than the standard threshold energy necessary to induce damage creation in binary elastic collisions, but due to the collective and coherent aspects of the process, the usual displacement energy threshold concept becomes inadequate. Molecular dynamics simulations have shown that lattice defects are, indeed, created when small amounts of kinetic energy are collectively given to the atoms located inside a cylindrical region around the projectile path. The energy deposition in electronic excitations, first, and the resulting damage, later, are strongly localized along the ion path, creating a particular damage pattern: the ion track [16].

In either picture (band or ionization), the relevant physical quantity to obtain is the force that the host nuclei are subjected to while the projectile moves in the system, especially those nuclei near the trajectory. From the point of view of the nuclei, viewed as a classical subsystem, the force is nonadiabatic since it depends on the history of the system including the electrons, which are continuously excited by the moving projectile. Therefore, the force will depend on the velocity of the projectile and time. Only when the projectile moves infinitely slow (effectively

$v \lesssim 0.2$ a.u., see below) the so-called adiabatic forces are indeed recovered.

Figure 3 shows the radial force on an Al target atom closest to the H projectile's trajectory as a function of position of the proton along its trajectory for different projectile velocities. The forces on the nuclei are calculated from the instantaneous (time-dependent) electron density as it would be obtained by expanding the Hellman-Feynman formula (but in this case, not applied to the ground state). At zero velocity we recover the adiabatic force, symmetric with respect to the H-Al distance with its maximum value at the closest approximation. As velocity increases, the shape of the curves acquires a complex structure that shifts the position of the maximum and eventually develops oscillations.

Above certain velocity and after the projectile passes, persistent oscillations of the force on the host atom appear in the simulation; the frequency of these oscillations is roughly ~ 0.8–$0.9 E_h/\hbar$ as given by simple Fourier analysis. This frequency can be compared to $\sim 0.81 E_h/\hbar$ (at the Brillouin zone border) of the natural plasma frequency of Aluminum as calculated via methods within the same density functional framework [39]. This is consistent with the picture that, only at high projectile velocities, plasmons (at finite excitation momentum q) can be produced and that these natural density oscillations persist with time. (Although, in this case, the persistence is enhanced by the periodic boundary conditions.)

To analyze the net effect of the forces on the host atoms, we evaluate the momentum transfer, as the integral of the force over distance, divided by the projectile velocity (v) (or equivalently as the integral of the force in time).

$$\Delta \mathbf{p} = \int \mathbf{F}(x(t))dt = \int \mathbf{F}(x)dx/v. \qquad (1)$$

When the initial thermal momentum of the target atom is small, the momentum transfer can be used to estimate the energy transfer to the target. When this is not the case, a full nuclear stopping cross section calculation is needed. Results in Fig. 4 on log-log scales show that for low velocities, up to about a tenth of the velocity corresponding to the maximum stopping (~ 1.5 a.u., from Fig. 2), the adiabatic approximation gives a good description of the momentum transfer, being proportional to $1/v$, up to 0.3 a.u.. However, as we approach the maximum on electronic stopping, a transition into a new regime is clearly seen where the momentum transfer passes through a minimum and goes into a plateau. This momentum transfer for high velocity (in a range of velocities from 0.3 to 2.0 a.u.) translates into an almost constant initial momentum change per target atom near the channel, independent of the projectile velocity, that can be several times the one that the adiabatic approximation will predict. This constitutes a coherent, uncompensated radial transfer of momentum. (From general arguments—see, e.g., Landau and Lifshitz's [40] discussion of momentum transfer in classical collisions—one expects a recovery of the $\Delta p \sim 1/v$ behavior at even higher v. It is, however, for velocities beyond the scope of this work.)

The effect described is neither equivalent to a thermal spike (random momentum gain) nor to a Coulomb explosion (atoms here are neutral and the origin of the force is not Coulombic between ions).

As far as we are aware, this result is new and provides a first principles calculation of the strength of the nonadiabatic effects on the distribution of the energy losses by an energetic projectile. Similar to the Coulomb explosion, this momentum transfer is radial outwards. However, it is not related to the ionization of the target atoms close to the projectile velocity but rather to the loss of the ability of electrons to provide chemical bonding as they become excited, an effect that starts to appear at velocities around 0.3 a.u., i.e., well below the maximum of $S_e(v)$ at 1.5 a.u. for the case of protons in Al.

These are the first steps towards the development of a unified first-principles simulation framework of the

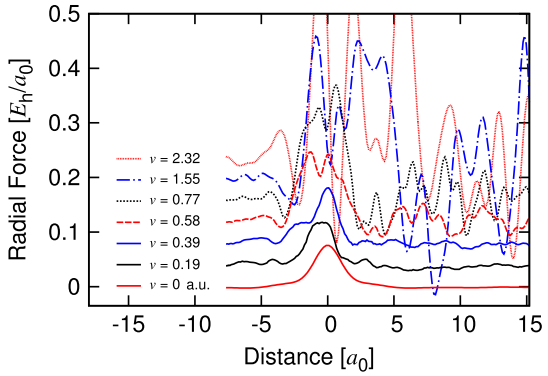

FIG. 3 (color online). Proton in aluminum: Radial force exerted on host atom (first neighbor to channel trajectory) vs. parallel distance to projectile at different projectile velocities v; $x = 0$ is the point of maximum proximity. The nonadiabatic curves have been shifted vertically for visualization purposes, but they all start with zero force.

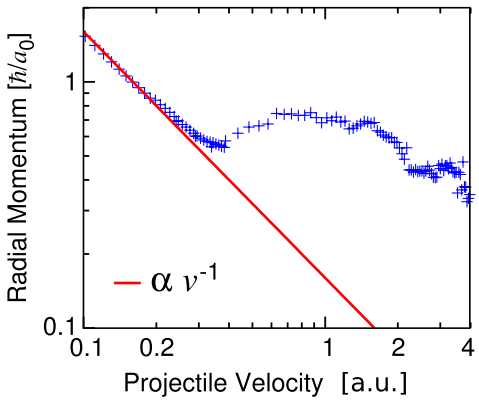

FIG. 4 (color online). Proton in aluminum: Radial momentum transferred to host atom vs. projectile velocity. The momentum transfer is calculated as the time integral of the force $\Delta p^{\perp}(v) = \int F_v^{\perp}(t)dt = \int F_v^{\perp}(x)dx/v$. At low velocity it tends to $\Delta p^{\perp}(v \to 0) = \int F^{\perp}_{\text{adiabatic}}(x)dx/v$.

electron-nuclear radiation damage problem, showing that it is feasible to include both the nuclear and electronic aspects of the problem. The implications for more accurate computer simulations of radiation damage are important. Recent work on band structure effects on the existence of a threshold velocity for the set up of electronic stopping (LiF, ices, etc.) [30,31] together with these results for high velocities highlight the limitations of the adiabatic and Langevin dynamics approximations and point toward the need of incorporating tractable forms for nonadiabatic effects into computer simulations of radiation damage in solids.

A. A. C. acknowledges that part of this work was performed under the auspices of the U.S. Department of Energy by Lawrence Livermore National Laboratory under Contract No. DE-AC52-07NA27344. D. S. P. acknowledges support from the Spanish MICINN (Project No. 2010-19609-C02-02). A. C. acknowledges support from the Center for Materials at Irradiation and Mechanical Extremes, an Energy Frontier Research Center funded by the U.S. Department of Energy (Award No. 2008LANL1026) at Los Alamos National Laboratory, and from the Laboratory Directed Research and Development Program. J. K. thanks Lawrence Livermore National Laboratory and the Department of Earth Sciences of the University of Cambridge for hospitality during the exploratory phase of this work and the Wellcome Trust for funding a sabbatical leave, during which this work was initiated.

[1] R. S. Averback and T. Diaz de la Rubia, in *Solid State Physics*, edited by H. Ehrenreich and F. Spaepen (1997), Vol. 51, p. 281.
[2] J. B. Gibson, A. N. Goland, M. Milgram, and G. H. Vineyard, Phys. Rev. **120**, 1229 (1960).
[3] M. Toulemonde, C. Dufour, and E. Paumier, Phys. Rev. B **46**, 14 362 (1992).
[4] T. Diaz de la Rubia, R. S. Averback, R. Benedek, and W. E. King, Phys. Rev. Lett. **59**, 1930 (1987).
[5] M. S. Daw and M. I. Baskes, Phys. Rev. B **29**, 6443 (1984).
[6] M. W. Finnis and J. E. Sinclair, Philos. Mag. A **50**, 45 (1984).
[7] M. Born and R. Oppenheimer, Ann. Phys. (Leipzig) **389**, 457 (1927).
[8] F. Seitz and J. S. Koehler, Solid State Phys. **2**, 305 (1956).
[9] I. M. Lifshitz, M. I. Kaganov, and L. V. Tanatarov, J. Nucl. Energy **A12**, 69 (1960).
[10] A. Caro and M. Victoria, Phys. Rev. A **40**, 2287 (1989).
[11] R. Fleischer, P. Price, and R. Walker, J. Appl. Phys. **36**, 3645 (1965).
[12] D. Lesueur and A. Dunlop, Radiat. Eff. Defects Solids **126**, 163 (1993).
[13] G. Schiwietz, P. Grande, B. Skogvall, J. P. Biersack, R. Köhrbrück, K. Sommer, A. Schmoldt, P. Goppelt, I. Kádár, S. Ricz *et al.*, Phys. Rev. Lett. **69**, 628 (1992).
[14] J. Rzadkiewicz, A. Gojska, O. Rosmej, M. Polasik, and K. Słabkowska, Phys. Rev. A **82**, 012703 (2010).
[15] C. Dufour, A. Audouard, F. Beuneu, J. Dural, J. P. Girard, A. Hairie, M. Levalois, E. Paumier, and M. Toulemonde, J. Phys. Condens. Matter **5**, 4573 (1993).
[16] E. M. Bringa and R. E. Johnson, Phys. Rev. Lett. **88**, 165501 (2002).
[17] D. M. Duffy and A. M. Rutherford, J. Phys. Condens. Matter **19**, 016207 (2007).
[18] F. Gygi and G. Galli, Phys. Rev. B **65**, 220102 (2002).
[19] D. Dundas, E. McEniry, and T. Todorov, Nature Nanotech. **4**, 99 (2009).
[20] R. G. Parr and Y. Weitao, *Density-Functional Theory of Atoms and Molecules (International Series of Monographs on Chemistry)* (Oxford University Press, New York, 1994), ISBN 9780195092769.
[21] C. C. Montanari and J. E. Miraglia, arXiv:0904.1386.
[22] M. Kitagawa and Y. H. Ohtsuki, Phys. Rev. B **9**, 4719 (1974).
[23] P. M. Echenique, R. M. Nieminen, and R. H. Ritchie, Solid State Commun. **37**, 779 (1981).
[24] M. Quijada, A. G. Borisov, I. Nagy, R. Diez Muiño, and P. M. Echenique, Phys. Rev. A **75**, 042902 (2007).
[25] I. Campillo, J. M. Pitarke, and A. G. Eguiluz, Phys. Rev. B **58**, 10 307 (1998).
[26] P. Sigmund, Bull. Russ. Acad. Sci. Phys. **72**, 569 (2008).
[27] O. Firsov, Sov. Phys. JETP **5**, 1192 (1957).
[28] J. P. Biersack and L. G. Haggmark, Nucl. Instrum. Methods **174**, 257 (1980).
[29] J. F. Ziegler, in *Nuclear Instruments and Methods in Physics Research Section B: Beam Interactions with Materials and Atoms* (2004), Vol. 219–220, p. 1027.
[30] J. M. Pruneda, D. Sánchez-Portal, A. Arnau, J. I. Juaristi, and E. Artacho, Phys. Rev. Lett. **99**, 235501 (2007).
[31] J. Kohanoff and E. Artacho, AIP Conf. Proc. **1080**, 78 (2008).
[32] J. M. Soler, E. Artacho, J. D. Gale, A. García, J. Junquera, P. Ordejón, and D. Sánchez-Portal, J. Phys. Condens. Matter **14**, 2745 (2002).
[33] A. Tsolakidis, D. Sánchez-Portal, and R. M. Martin, Phys. Rev. B **66**, 235416 (2002).
[34] W. H. Press, S. A. Teukolsky, W. T. Vetterling, and B. P. Flannery, *Numerical Recipes 3rd Edition: The Art of Scientific Computing* (Cambridge University Press, Cambridge, England, 2007), 3rd ed., ISBN 9780521880688.
[35] *Time-Dependent Density Functional Theory (Lecture Notes in Physics)*, edited by M. A. Marques, C. A. Ullrich, F. Nogueira, A. Rubio, K. Burke, and E. K. U. Gross (Springer, New York, 2006), 1st ed., ISBN .
[36] J. P. Perdew and A. Zunger, Phys. Rev. B **23**, 5048 (1981).
[37] I. Nagy and B. Apagyi, Phys. Rev. A **58**, R1653 (1998).
[38] V. U. Nazarov, J. M. Pitarke, Y. Takada, G. Vignale, and Y.-C. Chang, Phys. Rev. B **76**, 205103 (2007).
[39] A. A. Quong and A. G. Eguiluz, Phys. Rev. Lett. **70**, 3955 (1993).
[40] L. D. Landau and E. Lifshitz, *Mechanics, Third Edition: Volume 1 (Course of Theoretical Physics)* (Butterworth-Heinemann, Oxford, 1976), 3rd ed., ISBN 9780750628969.
[41] J. F. Ziegler (2011), http://www.srim.org/SRIM/SRIMPICS/STOP01/STOP0113.gif.